2

Methodology

In this chapter, the generally applicable fabrication procedures for the synthesis of perovskite solar cells (PSC) used in the thesis are outlined. More specialized procedures are described in the individual chapters of relevance. A brief description of the characterization techniques and analytical methods including X-ray diffraction, electron microscopy, UV-Vis and photoluminescence spectroscopy techniques and their working principles are discussed.

2.1 Perovskite solar cell preparation

The preparation of PSCs was carried out in accordance with standard procedures and involved the following processes:

I. Chemical etching of the fluorine-doped tin oxide (FTO) substrates
II. Deposition of the compact-TiO_2 layer
III. Deposition of the mesoporous-TiO_2 layer
IV. Deposition of SnO_2 film
V. Deposition of the perovskite layer
VI. Spin coating the HTM
VII. Thermal evaporation of electrode

I. Chemical etching of FTO substrate

Commercially available 10 cm x 10 cm sheets of FTO-coated glass were used as substrate (7 $\Omega\ cm^{-1}$, Nanoglobal). The required electrode pattern was obtained by masking off the desired areas of FTO with Kapton tape. The unmasked areas were then selectively etched away using a combination of Zn powder and a 4 M solution of HCl. Subsequent to this, the substrate was washed with laboline solution and then sonicated for 10 minutes in deionized (DI) water followed by boiling for 10 minutes. Later, the substrate was cleaned and sonicated in ultrasonic bath in the IPA for 10 minutes and then boiled for 10 minutes in IPA. The substrate was then dried with a nitrogen gun. After this, the substrate was then subjected to oxygen plasma cleaning for 15 minutes. This final cleaning step serves to remove any organic residues which may remain on the substrate.

Materials

All the chemical precursors were used as purchased without any further purification. Titanium (IV) isopropoxide (TTIP) (97%) and tin chloride ($SnCl_2$) (99.99%) were acquired from Sigma Aldrich. Formamidinium iodide (FAI) (99.99%), methyl ammonium iodide (MAI) (99.99%) and methyl ammonium bromide (MABr) (99.99%) were bought from Great cell solar (Australia). Lead iodide (PbI_2) (99%), 9,9′-spirobifluorene (Spiro-OMeTAD), bis(trifluoromethane)sulfonimide lithium salt (Li-TFSI), 4-*tert*-butylpyridine (TBP) (98%), dimethyl sulfoxide (DMSO) (99.5%), N,N-dimethylformamide (DMF) (99%) and chlorobenzene (CB) (99.8%) were bought from Sigma-Aldrich (USA) and Gold (Au) from hind high vacuum, Bangalore India. Microscopic glass slides (thickness 1.25 mm) purchased from Ms. Blue Star (Deluxe), Mumbai (India), were used for thin film deposition. In the present work, solution based spin coating and spray deposition route has been adopted for thin film deposition.

II. Deposition of the TiO_2 compact layer

Spray coating

Spray pyrolysis is a simple, cost-effective and solution-based deposition technique where the precursor solution is atomized and sprayed over a preheated substrate. The schematic of the spray pyrolysis is shown in **Figure 2.1**. The spray pyrolysis equipment consists of an atomizer, precursor solution, substrate heater, and temperature controller. Precursor atomization is the primary step for the deposition of a film on a substrate by spray pyrolysis. It involves the creation of aerosol of a precursor solution which is propelled with some initial velocity towards the heated substrate surface where the precursor reacts/decomposes. Spray pyrolysis generally uses pressurized air, ultrasonic, or electrostatic atomizers to create a spray of the solution.

The TiO_2 films were spray deposited utilizing a commercial spray pyrolysis system purchased from Holmarc Opto-mechatronics Pvt. Ltd. India. A schematic and photograph of the spray pyrolysis setup are shown in **Figure 2.1**. Titanium isopropoxide hereafter referred as TTIP (Sigma Aldrich, 90%) was used as a TiO_2 precursor. First, 10 ml isopropyl alcohol (IPA) was taken and stirred for 10 minutes, then TTIP (1 ml) was added dropwise and after 1 minute 1 ml acetyl acetone (AcAc) was added dropwise and kept for stirring for 2 hours at room temperature. After spraying the solution at 400ºC, the substrate was heated further for 30 minutes at 450°C and then cooled down normally [122]. The spray rate was controlled by a syringe pump (Unigenetics Instruments Pvt. Ltd., India). The speed of the spray nozzle was set as 200 mm/s in the x-direction and 2 mm/s in the y-direction while the precursor flow rate was 1 ml/min and the distance between the substrate and spray head nozzle was kept at ~12 cm. The nozzle pressure was adjusted to about 1 bar.

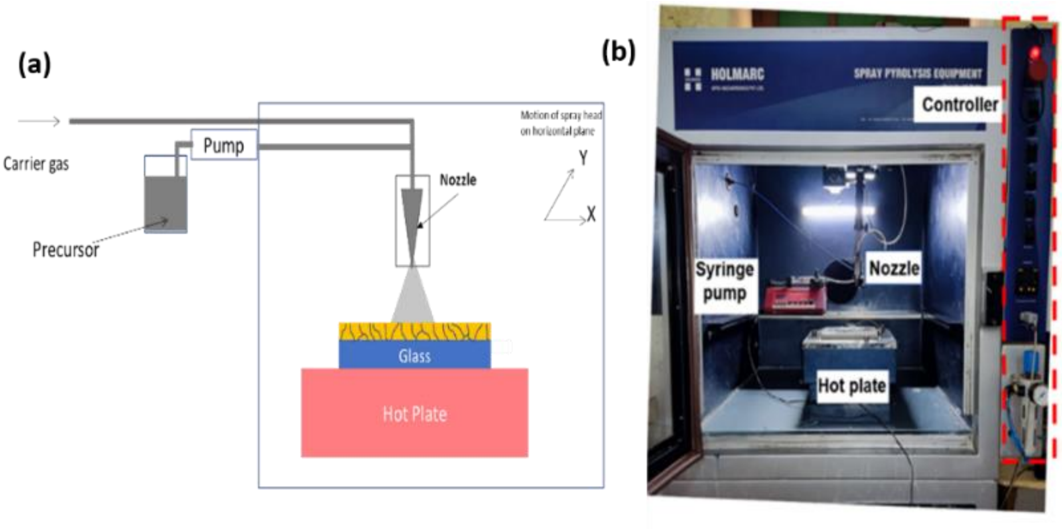

Figure 2.1 Schematic diagram and photograph of the spray pyrolysis setup.

Spin Coating

Spin coating is a common solution-based technique for processing thin films and coatings. When a precursor solution spins at high speeds, the centripetal force and the surface tension of the liquid together creates an even covering. The solvents are subsequently evaporated to form a film of thickness ranging from a few nanometres to a few microns [123]. Mesoporous TiO_2 (mp-TiO_2), perovskite and HTLs films were spin-coated utilizing a commercial programmable spin coating system (Model: spin NXG-P1A) purchased from Ms Apex instruments (Jadavpur, Kolkata, India). Solution for spin coating was prepared on magnetic stirring for optimum time and then spin coated on substrate, the spin coating instrument is connected with vacuum pump which creates vacuum during spin coating, setup for spin coating are shown in **Figure 2.2**.

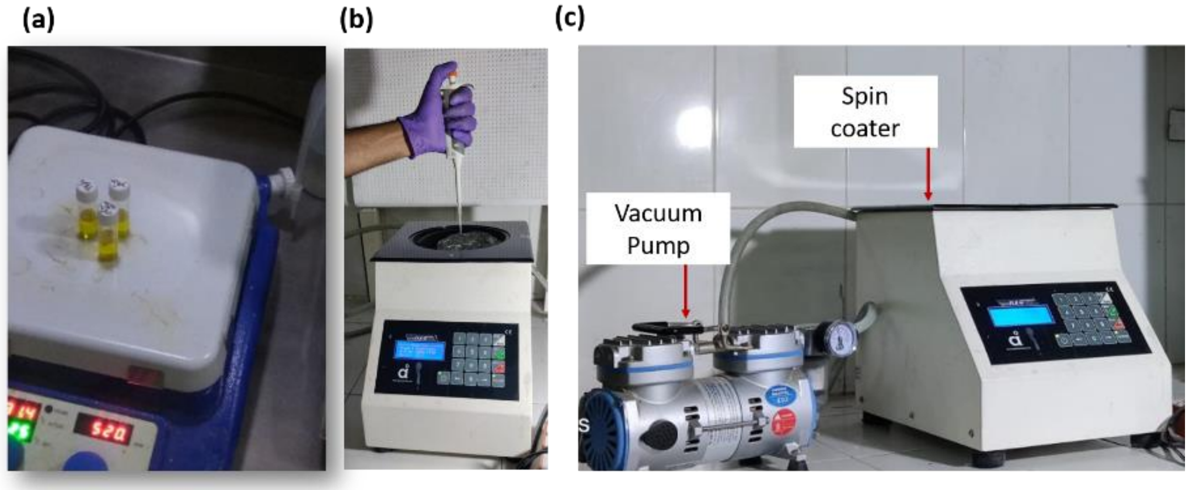

Figure 2.2 Photograph of a) solution preparation, b) spin coating of solution and c) spin coating set-up.

Deposition of the mesoporous TiO_2 layer

For mesoporous TiO_2 the commercially available TiO_2 paste (Dyesol 18NR-T) was spin-coated at 3000 r.p.m for 30 seconds, Dyesol paste was diluted in ethanol in a 1:6 weight ratio. After deposition of the TiO_2 paste, the substrates were then sintered to 500 ˚C for 30 minutes, after which they were cooled down normally before further processing.

III. Deposition of SnO_2 film

SnO_2 was used as an alternative to TiO_2 or in the case of bilayer TiO_2/SnO_2 ETL for efficient PSC. SnO_2 film was prepared by spraying the precursor solution prepared by dissolving 189 mg $SnCl_2$ (99.99%, Sigma Aldrich) in 10 ml methanol at 400°C followed by annealing at 450°C for 30 minutes.

IV. Synthesis of the perovskite layer

Perovskite layer ($FA_{0.75}MA_{0.25}Pb(BrI)_3$) was spin coated the precursor solution prepared by mixing 129 mg FAI, 27 mg MABr and 461 mg of PbI_2 (Sigma Aldrich) in the mixture (4:1) of DMF and DMSO (Sigma Aldrich). Three-step spin coating process: 500 rpm for 10 s, 1500 rpm for 15 s, and 3000 rpm for 30 s, were followed, and during the last step, 100 µl CB were dripped as an antisolvent [68] and then annealed at different temperature and time on a hotplate and rapid thermal processing (RTP) for comparative study.

The perovskite film ($FA_{0.5}MA_{0.5}PbI_3$) was prepared by mixing 86 mg of formamidinium iodide (FAI, Great cell solar), 79 mg of methylammonium iodide (MAI, Great cell solar), and 461 mg lead iodide (PbI_2, Sigma Aldrich, 99%) in a mixture of DMSO and DMF (1:4) was spin-coated by three-step spin coating process: 500 rpm for 10 s, 1500 rpm for 15 s, and 3000 rpm for 30 s, and during the last step, 100 µl CB were dripped as an antisolvent, then annealed at 100°C for 10-30 minutes on a hotplate.

Similarly, $FASnI_3$ perovskite film was coated on the mp-TiO_2 coated substrate in argon glove box. The precursor solution was prepared by adding 372 mg SnI_2 (Sigma Aldrich) 15.6 mg SnF_2 (Sigma Aldrich) or 18.5 mg $SnCl_2$ (Sigma Aldrich) in 0.8 ml DMF and 0.2 ml DMSO (Sigma Aldrich). The precursor solution was spin-coated on the m-TiO_2 at 500 rpm for 10 s, 1500 rpm for 15 s and 3000 rpm for 30 s and annealed at 100 °C for 20 minutes. In order to improve the microstructure antisolvents CB, and toluene (100 µl) were dripped during the 3rd spinning step.

V. Spin coating the HTL

Hole transport layer ie Spiro-OMeTAD solution was prepared by dissolving 72.3 mg of Spiro-OMeTAD, 29 µL of 4-tert-butyl pyridine, (TBP) and 18 µL of lithium bis(trifluoromethane sulfonyl)imide (Li-TFSI) (520 mg Li-TFSI in 1 mL acetonitrile, 99.8%, Sigma-Aldrich) in 1 mL of chlorobenzene (99.9%, Sigma Aldrich). The solution was spin coated at 4000 r.p.m for 30 seconds. After the spin coating of Spiro-OMeTAD, the coated sample was taken out from the glove box and kept inside a box along with some silica gel for oxidation. The oxygen was supplied through a hole for 10 minutes and then sealed properly. The box was kept out for 12 hours for complete oxidation. For copper thiocyanate (CuSCN) as HTL the solution was prepared by adding 15 mg of CuSCN in 1 ml of dipropyl sulphide (DPS) and kept for stirring overnight. And then coated on perovskite layer by taking 80 µL solution and spin coated at 3000 r.p.m for 30 second then finally annealed at 65° C for 10 minutes.

VI. Thermal evaporation of electrode

Thermal evaporation is one of the simplest form of physical vapour deposition technique for the deposition of thin electrode layers that involve heating of target material via applying electric current, the required material evaporates in a high vacuum due to high-temperature heating, which enables the direct deposition of vapour molecules/atoms over the substrate on which the vapour phase again condenses as a thin film [124]. Here, the 90-100 nm thick gold electrical front contact was deposited over the HTL by thermal evaporation under a high vacuum (10^{-6} mbar) through a shadow mask, the photograph of thermal evaporation system is shown in **Figure 2.3,** whereas the photograph of the complete device on small and bigger substrate is represented in **Figure 2.4.**

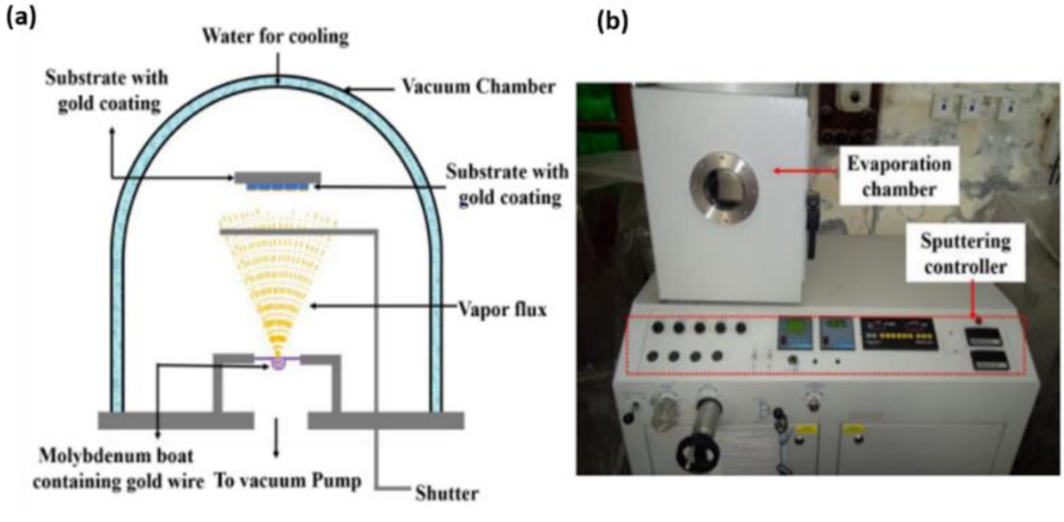

Figure 2.3 a) Schematic showing the thermal evaporation, and b) photograph of thermal evaporation system.

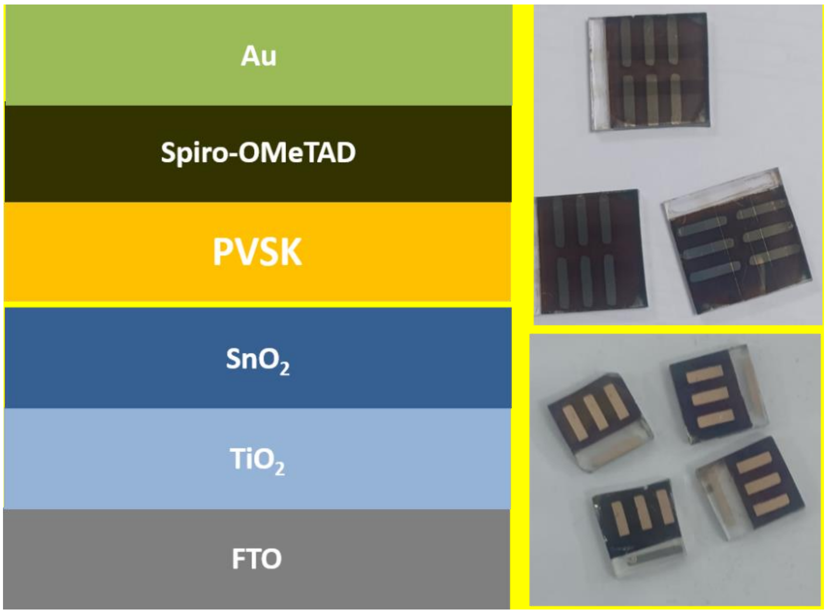

Figure 2.4 a) Schematic showing cell architecture and b) photograph of the cells.

2.2 Material Characterization

2.2.1 X-ray diffraction (XRD)

X-ray diffraction is a common and rapid analytical technique for the study of crystal structures and atomic spacing. It is primarily used for crystallographic phase identification and phase quantification of crystalline material providing information on unit cell dimensions. XRD is based on constructive interference of monochromatic X-rays, a cathode ray tube, filtered to produce monochromatic radiation, collimated to concentrate, and directed toward the sample, generates these X-rays [125]. Diffraction peaks are generated when a beam of X-ray incident (of wavelength λ) on a crystalline material satisfies the Bragg condition i.e. $n\lambda = 2d_{(hkl)}Sin\theta$, where 2d($hkl$) is the interplanar spacing of (hkl) planes. The XRD patterns generated, deliver a unique “fingerprint” for crystallographic phase information. The XRD patterns were recorded utilizing a diffractometer Rigaku Mini flex-600 (40 kV–15 mA); in Rigaku, Tokyo, Japan using CuKα radiation ($\lambda = 0.154060$ nm). XRD data were recorded in the 2θ scan ranging from 10 to 70° at a step size of 0.02° with a scan rate of 5°/min **(Figure 2.5).**

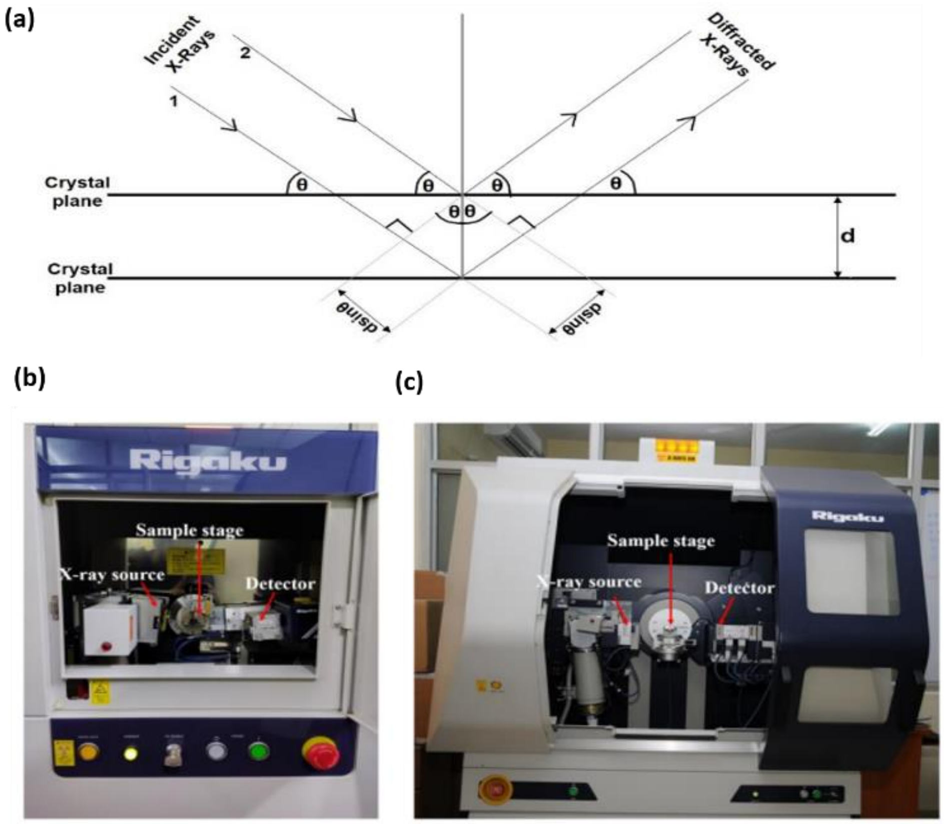

Figure 2.5 a) Schematic diagram of Bragg’s law, b) photograph of bench top XRD image, c) photograph of the front view of GIXRD.

2.2.2 Field emission Scanning electron microscope (FESEM)

FESEM is the most widely used electron microscope which examines microscopic structure by scanning the surface of materials, similar to scanning confocal microscopes but with much higher resolution and much greater depth of field [126]. FESEM consists of an electron gun at the top as a source of the electron beam with energy ranging from a few hundred eV to a few keV. The electrons are converged to form a fine probe of diameter < 5 nm through the electromagnetic lenses. The sample is scanned by rastering of electron beam over the sample surface using the scan coils. The high energy electrons penetrate the surface of the specimen and undergo elastic and inelastic interactions generating a series of signals including secondary electrons, backscattered electrons, characteristics X-rays and bremsstrahlung radiation. While secondary electrons are used for imaging surface topography, phase identification, while compositional contrast can be obtained from backscattered electrons. Energy dispersive X-ray spectroscopy (EDX) attached to FESEM is utilized to obtain elemental composition using the emitted characteristic X-rays. The FESEM model Nova Nano SEM 450, supplied by FEI Company of USA (S.E.A.) PTE, LTD was utilized for imaging, while the energy-dispersive X-ray spectra of the perovskite film were acquired utilizing a customary unit (Pegasus Integrated EDS-EBSD with Octane Plus and Hikari Pro, EDAX Inc.) attached to the FESEM (**Figure 2.6**).

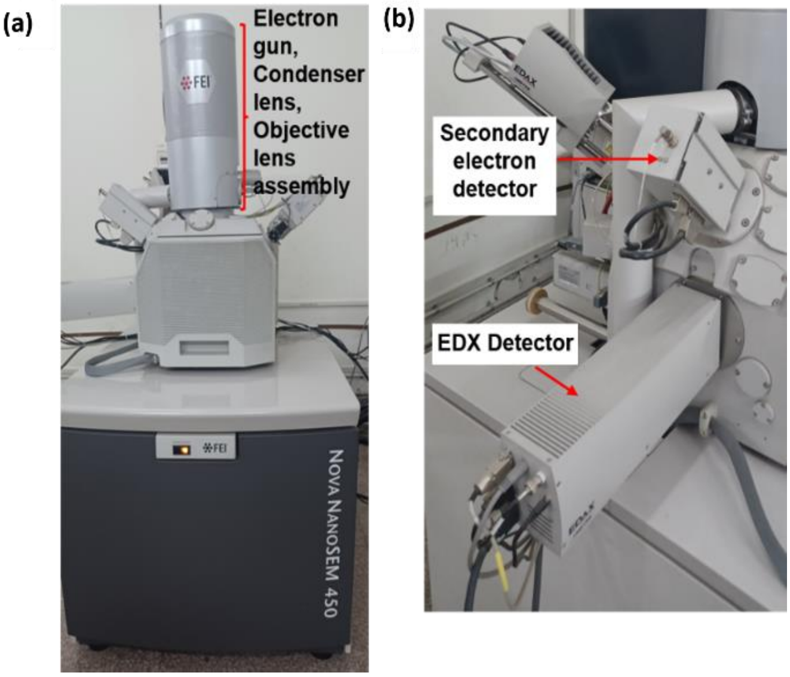

Figure 2.6 Photograph showing a) front view of FESEM and b) side view of FESEM.

2.2.3 UV Vis Spectroscopy (UV Vis)

UV-Visible (UV-Vis) is used to perform absorption and reflectance using light in the visible and adjacent ranges, where wavelengths/energy of UV or visible light that are absorbed by or transmitted through the sample is measured in comparison to a reference blank sample. It generally operates in the 300 to 1100 nm wavelength range. In the present work, UV–Vis/NIR spectrometer, JASCOV-770, USA was used to identify the absorbance and bandgap of the perovskite absorber layer, TiO_2 and SnO_2. Bandgap was determined by Tauc plot assuming that perovskite film is a direct bandgap material **(Figure 2.7).**

The following relation expresses the energy-dependent absorption co-efficient

$$(\alpha . hv)^{\frac{1}{n}} = A\left(hv - E_g\right) \qquad 2.1$$

where α is the absorption coefficient, h is Planck's constant, v is the frequency of photon, E_g is the optical bandgap, n is a factor that has values 2 or ½ for the indirect or direct nature of electron transition, and A is the slope of the Tauc plot in the linear region respectively. The basic method for finding bandgap from Tauc plot is to obtain optical absorbance of the sample in a range of energies from below the band gap transition to above it. $(\alpha h v)^{1/n}$ is plotted against (hv) to test the value of n to which provides the best fit and thus identifies the nature of transition while the energy-axis intercept gives the band gap value (E_g). In this case, it might be possible to extract both indirect and direct edges with plots using the appropriate exponents [127].

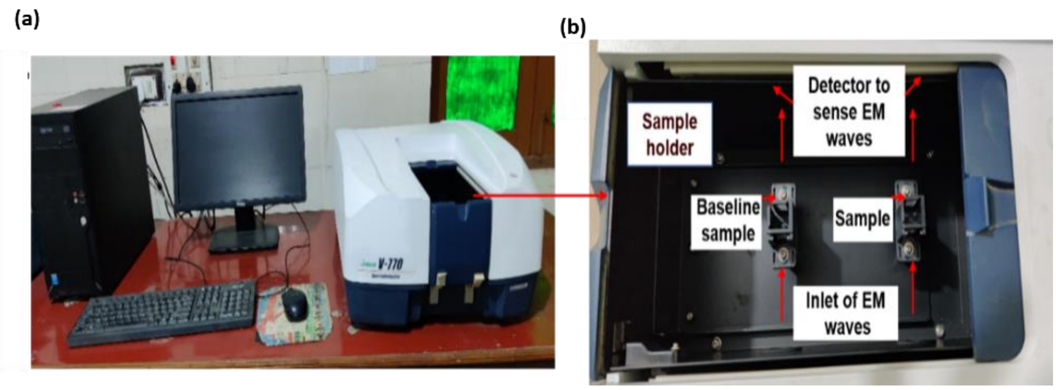

Figure 2.7 Photograph of a) UV VIS spectroscopy setup and, b) sample holder chamber.

2.2.4 Photoluminescence (PL) spectroscopy

Photoluminescence spectroscopy (PL) is a contactless, non-destructive method of probing the electronic structure of materials. It is based on the photoluminescence process *i.e.* the emission of light from a material following the absorption of light. Quantum mechanically, this can be described as an excitation to a higher energy state and then return to a lower energy state accompanied by the emission of a photon. If a light particle (photon) has an energy greater than the band gap energy, then it can be absorbed and thereby raise an electron from the VB up to the CB across the forbidden energy gap. In this process of photoexcitation, the electron generally has excess energy which it loses before coming to rest at the lowest energy in the CB. At this point, the electron energy eventually falls back down to the VB. As this happens, the energy it loses is converted back into a luminescent photon which is emitted from the material. Thus the energy of the emitted photon is a direct measure of the band gap energy, E_g. The process of photon excitation followed by photon emission is called photoluminescence **(Figure 2.8a).** The PL spectrometer primarily has a source of light, monochromators, a sample holder and a detector shown in **Figure 2.8 b-c**.

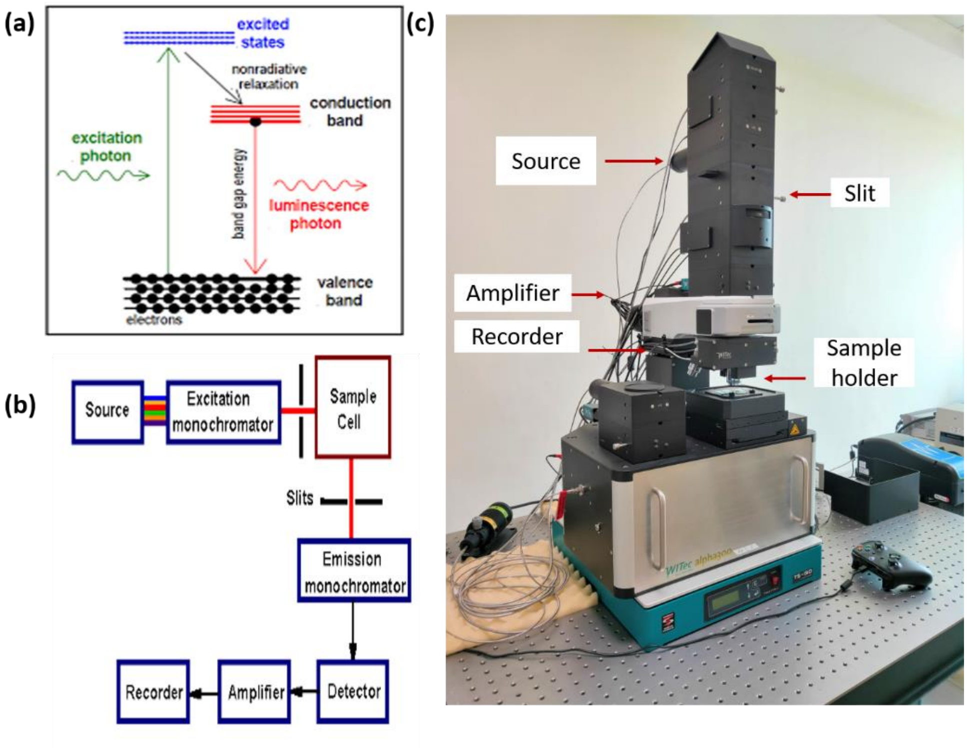

Figure 2.8 a) Schematic of the a) principle of photoluminescence and b) instrumentation and c) Photograph of PL and TRPL set-up.

2.2.5 Time –resolved Photoluminescence (TRPL)

Time-resolved photoluminescence (TRPL) spectroscopy is a powerful technique that has been employed to study charge carrier recombination kinetics of semiconductors and photo-luminescent materials. TRPL measures the radiative electron-hole recombination after absorption of a short light excitation pulse (typically of the order of the ns or ps). TRPL is usually measured using time-correlated single photon counting (TCSPC) in which the sample is periodically excited by a pulsed laser and the sample emission is measured at the desired wavelength. TRPL decays have been usually fitted to bi-or tri-exponential fit according to **Equation 2.2** to deduce lifetime components τ_1 and τ_2, as well as the amplitudes A_1 and A_2, the average lifetime can be calculated by **Equation 2.3** [128].

$$f(t) = \sum_i A_i \exp(-t/\tau_i) + K \tag{2.2}$$

$$\tau_{ave} = \frac{\sum A_i \tau_i^2}{\sum A_i \tau_i} \tag{2.3}$$

To study the charge, transfer properties, steady state photoluminescence (PL) and time-resolved photoluminescence (TRPL) were measured using a pulse diode laser (λ_{exc}=405 nm) as an excitation source (Witech alpha 300 RA/S (Germany) **(Figure 2.8c).**

2.3 Solar cell Characterization

Solar cell performance parameters were measured under simulated AM 1.5G illumination provided by a solar simulator. A source meter (Keithley 2400, USA) was used to record the current-voltage characteristics. All solar cells were masked with a metal aperture which was used to define the active area of the devices, which in this case was 0.06 cm^2 and 0.01 for small (1.5 cm x 1.5cm) and big (2.5 cm x 2.5 cm) substrate respectively. This masking is essential to eliminating any possible edge effects which may contribute to the measured current densities. A solar simulator is a controllable indoor test facility that provides illumination approximating natural light for the testing of PSC devices. The solar simulator provides continuous illumination (Xenon lamp) in time with an intensity of 100 mW/cm^2. The solar simulator (Model: #SS30AAA, Photo-Emission Tech., USA) is utilized to measure the J-V curve using a Keithley 2450 source meter, along with the conversion efficiency, maximum power output, fill factor, series resistance, resistivity and shunt resistance of solar cells and other materials and devices. Voltage was scanned in the range of -1V to 1V, with voltage compliance of 1A. J-V curves were plotted using Origin Labs software **(Figure 2.9).**

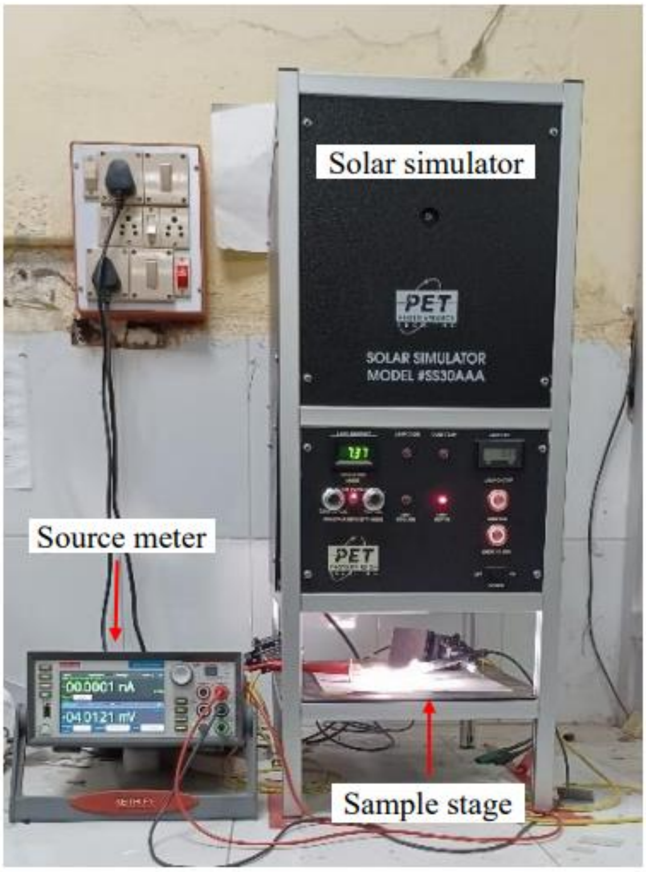

Figure 2.9 Photograph showing the set-up for I-V measurement.